# Post-Helene Change Detection Assessment using Remote Sensing Images in North Carolina

Rizwan Ahmed Ansari [1], Timothy Mulrooney [1], Zakariya Ansari [2]

[1] Department of Environmental, Earth and Geospatial Sciences, North Carolina Central University, USA – ransari@nccu.edu, tmulroon@nccu.edu
[2] Savitribai Phule Pune University, Pune, India – mails2zakariya@gmail.com

**Keywords:** Hurricane Helene, change detection, remote sensing, spectral indices, damage assessment

**Abstract**

The occurrence of hurricanes in the Southern U.S. is increasingly frequent, and assessing the damage caused to forests is essential for implementing protective measures and comprehending recovery dynamics. This work aims to create a data integration framework utilizing LANDSAT 8 and geographic information system (GIS) data for change detection analysis. We propose a composite spectral index method along with univariate difference imaging and ISO data clustering techniques to create a change detection map reflecting disturbances in regions of McDowell County in North Carolina affected by Hurricane Helene. Accuracy assessment is conducted with GIS data and maps from the National Land Cover Database. The proposed technique demonstrated commendable performance, with overall accuracy ranging between 64% and 86% and kappa statistics spanning from 0.2 to 0.64. The results demonstrate a fair correlation with GIS data and can be utilized to evaluate damage severity.

## 1. Introduction

Natural hazards can destroy buildings, damage forest ecosystems, and cause agricultural losses due to flooding, as well as indirect effects far from the event's epicenter. Despite being far inland from coastal areas that generally show the most damage, weakening storms or their remnants have historically flooded and destroyed western North Carolina. On September 26, 2024, category 4 Hurricane Helene hit Florida's Gulf Coast with 140 mph winds. Helene arrived in North Carolina on September 27, 2024, after heavy rain in the west (Cooper, 2024). Traditionally, field visits are used to collect questionnaires, interviews, and photos for preliminary damage and loss assessments. Depending on the damage and accessibility, gathering complete information can take days or weeks. Thus, improved robust methods for rapid and efficient damage loss estimation are crucial.

The remote sensing methodology employing change detection algorithms and vegetation indices has been demonstrated in numerous studies to be a powerful tool for large-scale evaluation of forest disturbances (Zhao et al., 2024; Pulvirenti et al., 2020). Change detection in remote sensing is utilizing two or more aerial or satellite imageries of the same geographic area to identify changes in land use and land cover characteristics across time (Kuzu et al., 2024; Lu 2025; Rynkiewicz et al., 2025). Most established change detection techniques rely on per-pixel classifiers, including the post-classification comparison method, and utilize pixel-based change information in the spectral domain of the images (Wu et al., 2021; Lv 2018; He et al. 2024). To identify changes from pixel-based change data in images, change detection methods, such as univariate image differencing (UID), are necessary.

Numerous studies have depended on satellite remote sensing, employing variations in diverse vegetation indices as indicators of impacted regions, with scant efforts to evaluate their quantitative relationship with landcover damage at the pixel level and few comparative analyses concerning their effectiveness (Salim et al. 2024, Jing et al. 2025, Zhou et al. 2023). Landsat datasets were employed for quantitative evaluations of vegetation dynamics and cyclone damage to arid forests (Singh et al. 2024). Change detection methods often involve the preparation of satellite imagery, feature extraction, the implementation of change detection methodologies, and the assessment of accuracy. Image preprocessing generally entails a series of operations, such as mitigating atmospheric effects on radiance, accurate image registration, extraction of areas of interest, and transformation of images into indices that demonstrate a strong correlation between their values and land cover characteristics.

Spectral indices have been computed by basic band arithmetic procedures, utilizing the distinct reflectance patterns of certain land cover and use objects across various energy spectrum. The prevalent indicators in remote sensing change detection include the normalized difference vegetation index (NDVI), the ratio of near-infrared to red image (RVI), the Tasseled Cap index of greenness (TCG), the Tasseled Cap index of wetness (TCW), and the soil-adjusted vegetation index (SAVI). The indices can assess the presence and density of green vegetation, overall reflectance, and soil moisture content and vegetation density (Rouse et al., 1974). NDVI, with a value range from −1 to +1, is likely the most often utilized metric for identifying both seasonal variations in green biomass and alterations due to human activities and natural disturbances. The NDVI distinguishes green vegetation from other surfaces due to chlorophyll absorption in the red band and reflection in the near-infrared band. Consequently, high NDVI values signify substantial leaf biomass, canopy closure, leaf area, and the quantity of photosynthetically active green biomass (Rouse et al., 1974). NDVI is unable to distinguish between very dense and dense canopies because of the restricted penetration ability of reflected red spectra, a phenomenon known as the saturation problem. The saturation issue of NDVI may restrict its capacity to identify comparatively little damage in densely populated forests (Rouse et al., 1974). RVI, a ratio-based vegetation index, closely resembles NDVI but exhibits more sensitivity to dense forest. RVI exhibits the greater sensitivity at higher leaf area index values (Coppin et al., 2004). SAVI is a transformation method that reduces the impact of soil brightness on spectral vegetation indices, including red and near-infrared wavelengths like NDVI and RVI (Coppin et al., 2004). The application of SAVI can considerably reduce the estimation of vegetation covering induced by soil brightness, in contrast to NDVI, particularly when vegetation cover is low (Coppin et al., 2004).

This contribution has been peer-reviewed. The double-blind peer-review was conducted on the basis of the full paper.
https://doi.org/10.5194/isprs-annals-X-5-W2-2025-23-2025 | © Author(s) 2025. CC BY 4.0 License.

Researchers have employed TCW to assess the age and structural complexity of mature and old-growth forest stands and to identify change in forests resulting from mortality and timber harvesting (Crist et al. 1986). The assessment of vegetation water content generally employs signals from liquid water absorption channels in the short wave infrared (SWIR) spectra, contrasted with signals from channels that are insensitive to liquid water in the NIR spectra. Numerous indices utilizing SWIR and NIR reflectance have been established, including normalized difference water index (NDWI) (Gao and Cao, 1996).

This study is based on our published work (Ansari et al., 2025) and aims to investigate the effectiveness of common spectral indices in detecting post-hurricane damage and to use GIS data for evaluating damage severity in hurricane-affected areas. The specific objectives of this study are to (1) identify a composite set of reliable indices to detect affected regions and assessing damage severity, (2) implement and analyze a methodology for rapid post-hurricane damage assessment, and (3) validate this methodology using independent GIS data.

## 2. Study Area and Datasets

The study area covers McDowell County, located within the southern Appalachian Mountains region in the western part of North Carolina, USA (Figure 1). Forest in this county covers roughly 75% of the total area of 445 square miles (United States Census Bureau, 2024). Two Landsat-8 images were collected; the first was taken on August 30, 2024, before Hurricane Helene hit, and the second was taken on October 17, 2024. All the spectral indices were derived from these two images. It was assumed that during this short period of time, no other disturbances occurred in the study area other than the damage from Helene. It was also assumed that the changes detected by the change detection techniques were a direct result of the hurricane's impacts.

To facilitate the image processing and execute change detection techniques, two more sets of geographically referenced data were gathered: (1) a GIS data layer from NHQRedCrossGIS (NQRedCrossGIS, 2024) as shown in Figure 2, and 2018 TIGER/Line shapefiles from the Environment Systems Research Institute and (2) Training and validation samples were collected from National Land Cover Database (NLCD) class maps Annual NLCD-2023 (NLCD, 2024). Data processing and analysis were carried out in ArcGIS Pro 3.3.

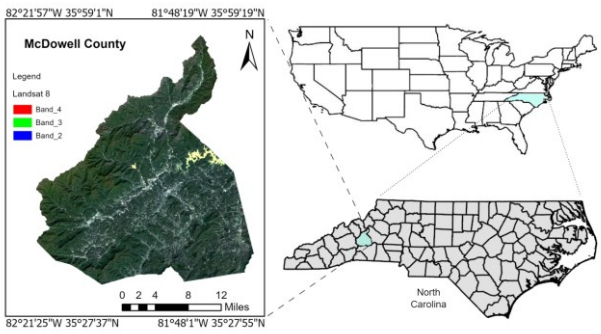


Figure 1. Geographical location of the study area.

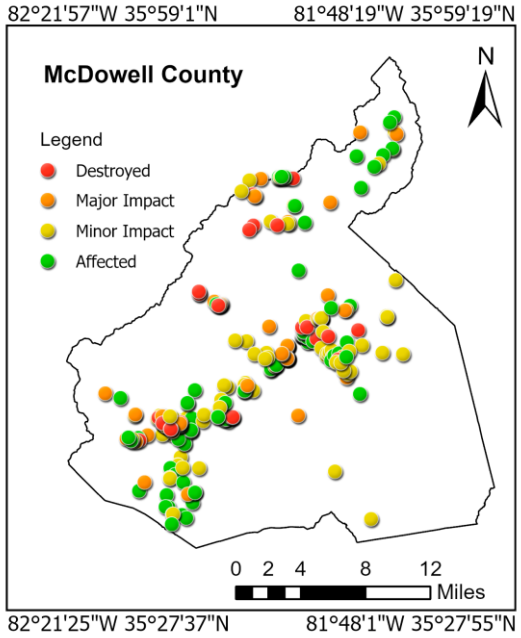


Figure 2. GIS Datapoints (adapted from [NQRedCrossGIS, 2024]).

## 3. Methodology

To achieve its objectives, this study was conducted with the workflows in Figure 3. The main steps include: (1) data collection, including training and validation data, Landsat 8 images, and other assisting data; (2) Landsat images preprocessing; (3) masking out the non-forest area; (4) calculating spectral indices; (5) implementation of the UID method to detect forest damage; (6) validations for the derived forest damage; and (7) producing and analyzing the final products.

Spectral indices (SI) including NDVI, TCG, TCW, RVI, SAVI, and NDWI are calculated from Landsat dataset using the equations provided in Table 1. The adjustment factor (L) in the SAVI equation was set at 0.5. Designating L as 0.5 accurately reflects the average intermediate density of the region's forests. Increment in L beyond 0.5 would amplify soil background effects in SAVI (Coppin et al. 2004).

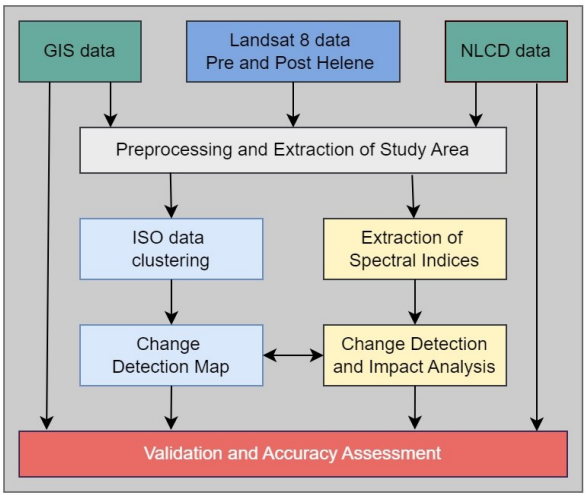


Figure 3. Proposed Methodology.

This contribution has been peer-reviewed. The double-blind peer-review was conducted on the basis of the full paper.
https://doi.org/10.5194/isprs-annals-X-5-W2-2025-23-2025 | © Author(s) 2025. CC BY 4.0 License.

| SI | Equations in terms of bands of Landsat 8 |
|---|---|
| NDVI | (B5-B4)/(B5+B4) |
| SAVI | (B5-B4)(1+L)/(B5+B4+L) |
| RVI | B5/B4 |
| TCW | 0.1509.B2+0.1973.B3+0.3279.B4+0.3406.B 5-0.7112.B6-0.4512.B7 |
| TCG | -0.2848.B2-0.2435.B3- 0.5436.B4+0.7243.B5+0.084.B6-0.18B7 |
| NDWI | (B5-B6)/(B5+B6) |

Table 1. Spectral Indices

Forested land regions prior to Helene were detected via the ISODATA clustering method for unsupervised classification based on the image from 30 August 2024. The imagery was categorized into 20 classifications, including deciduous, evergreen, and mixed forests, corresponding to the twenty classes of NLCD land cover data. The imagery was subsequently grouped into three categories utilizing the signature file and visual inspection. Only the categories identified as forests or those potentially qualifying as forests were carefully analyzed, assessed, and categorized through visual inspection of the NLCD. The obtained forestland imagery was used as a mask for continuous change images and was utilized as reference data in identifying forest disturbances.

The generation of continuous change imagery by the UID algorithm was performed by subtracting the spectral index (SI) imagery post-Helene from pre-Helene, by which the differences in the spectral responses to hurricane damage were emphasized. The spectral index changed detection map is calculated as

$$\Delta SI = \frac{\left(SI_{pre-Helene} - SI_{post-Helene}\right)}{SI_{pre-Helene}} \quad (1)$$

In an optimal scenario, if forest cover was modified by Helene, UID should produce a continuous change imagery where higher magnitude values indicate disturbed forests, while zero or close-to-zero values denote undisturbed forests.

A variety of methodologies have been developed for detecting land cover changes in continuous change imagery. These methodologies identify land cover changes based on threshold values established either automatically using specific algorithms or through manual trial-and-error methods, which are complex to implement and may compromise both the accuracy and dependability. This study employed Natural Breaks (Jenks) in ArcGIS Pro to categorize the changed images to account for non-uniform distributions. The percentage of affected area was calculated for individual and various combinations of ΔSI to evaluate the degree of impact. The contribution of each spectral index in the change detection map was analyzed in terms of statistical distribution. The mean of ΔSI, shift amplitude (SA), statistical dispersion in terms of interquartile range (IQR) were utilized to assess the accuracy of the change detection map. The change detection maps were examined using the GIS data layer from NHQRedCrossGIS for various severity levels.

ISODATA clustering produced two classification maps (Mpre and Mpost) with three categories (forest, water, and built-up regions) based on pre- and post-Helene processed Landsat images. Validation was conducted on the Mpre map utilizing NLCD-2023 data to accurately classify various categories within the study area. A change detection map was produced from the two classification maps and compared with the maps created using ΔSI tiles. An independent cross-validation followed by accuracy assessment was conducted by analyzing changed and unchanged pixels from the change detection maps in terms of user's accuracy (UA), producer's accuracy (PA), overall accuracy (OA), and kappa statistics (KS).

## 4. Results and Analysis

Figures 4 and 5 illustrate the change maps generated by various spectral indices. The overall accuracies and KS values of the classification ranged from 60.21% to 86.53% and from 0.2461 to 0.7425, respectively (Table 2). The UID with the composite index signature appeared as the most promising method, exhibiting the best overall accuracy and KS. The overall accuracies and KS values of the three vegetative indices—NDVI, RVI, and SAVI—were comparable. The accuracies attained by NDWI and TCW were comparable, ranging narrowly from 75.02% to 77.98%. Despite a strong association between NDVI and RVI, RVI demonstrated superior efficacy in identifying affected areas.

| SI | UA (%) | PA (%) | OA (%) | KS |
|---|---|---|---|---|
| NDVI | 65.78 | 78.69 | 70.92 | 0.4012 |
| SAVI | 67.92 | 84.32 | 72.18 | 0.4132 |
| RVI | 66.24 | 82.95 | 71.82 | 0.4082 |
| TCG | 56.70 | 52.86 | 60.21 | 0.2461 |
| TCW | 80.95 | 78.10 | 75.02 | 0.6035 |
| NDWI | 83.10 | 85.95 | 77.98 | 0.6419 |
| Composite index | 91.87 | 92.52 | 86.53 | 0.7425 |

UA: User's Accuracy, PA: Producer's Accuracy, OA: Overall Accuracy, KS: Kappa Statistics

Table 2. Accuracy Assessment

Of all the individual indices analyzed in this study, change detection using NDWI achieved the highest accuracy (77.98%), demonstrating that NDWI effectively captured forest changes caused by Hurricane Helene to the greatest extent. The composite SI recorded forest changes with an overall accuracy of 86.53% and a KS of 0.7425.

To effectively illustrate the efficacy of our suggested method, samples of varying severity levels and validation points derived from GIS data are presented in Figure 6. The pixels denoting destroyed regions, together with those exhibiting significant and small damages, are discovered and analyzed in relation to the pre- and post-Helene sample tiles and the associated changes in the change detection map, alongside the GIS data points. The change map results align with the GIS data points as indicated in red, orange and yellow points in row 1, 2 and 3 respectively (Figure 6). The impacted areas indicated by the proposed composite indices turned out to be more consistent with different damage severity (Table 2).

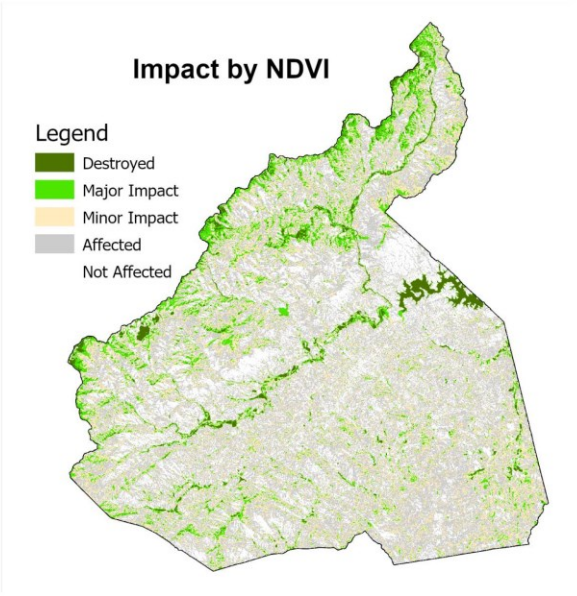


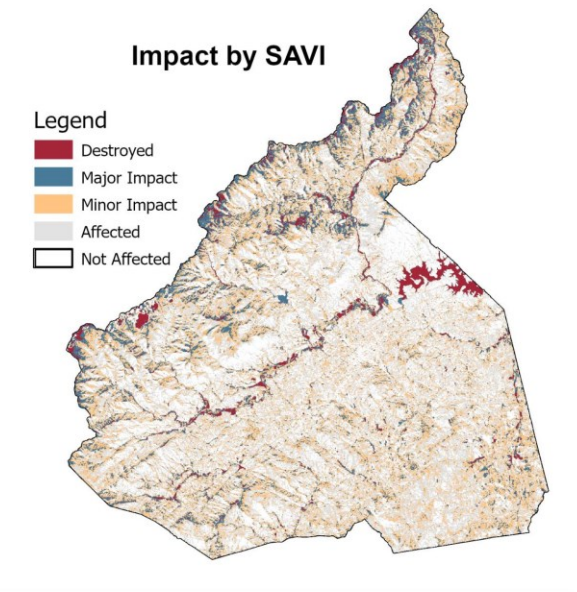


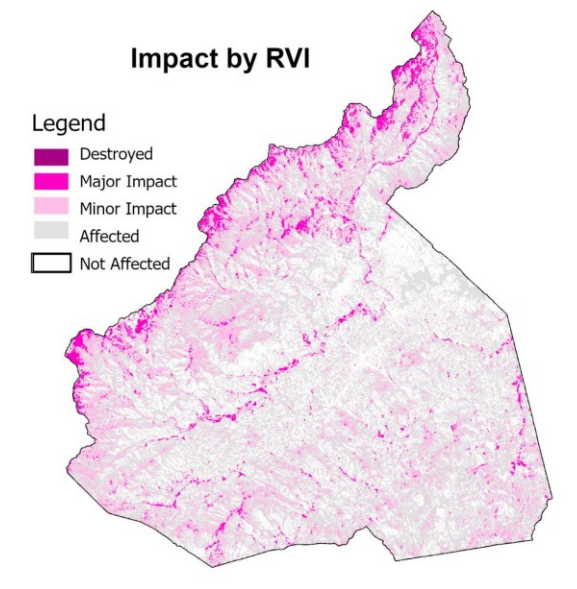


Figure 4. Change Detection Maps.










Figure 5. Change Detection Maps.

This contribution has been peer-reviewed. The double-blind peer-review was conducted on the basis of the full paper.
https://doi.org/10.5194/isprs-annals-X-5-W2-2025-23-2025 | © Author(s) 2025. CC BY 4.0 License.

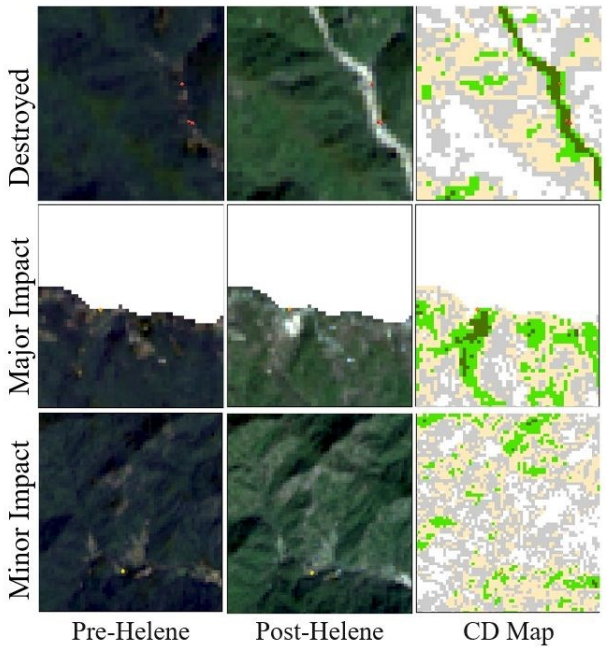


Figure 6. Overlay of GIS datapoints on CD map; red (in the first row), orange (in the second row) and yellow (in the third row) GIS datapoints indicate destroyed, major impact and minor impact pixels.

The area and spatial distributions of forests affected by Hurricane Helene differed according to the spectral indices (Table 2; Figures 4-6). Figure 7 illustrates the contribution of various indices to the identification of damage levels. NDVI, NDWI, and SAVI are the indices that identify the most significant effects. These indices appear to be the most responsive in identifying substantial damage in forested regions. RVI identifies the least affected areas, indicating a greater emphasis on recognizing regions that remain unimpacted, but its detection of severe consequences is comparatively diminished. TCG is more focused on minor impact areas and detects fewer severe impacts.

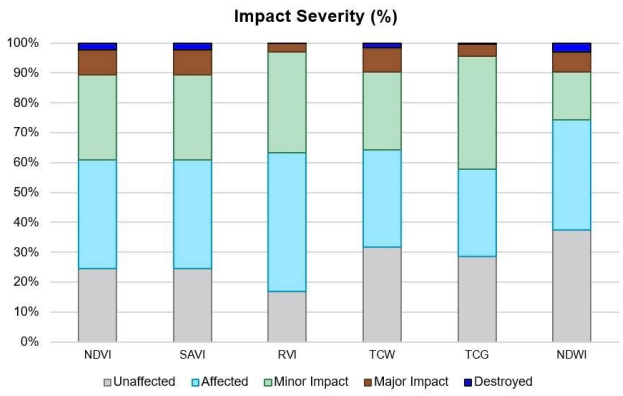


Figure 7. SI contibution in impact severity

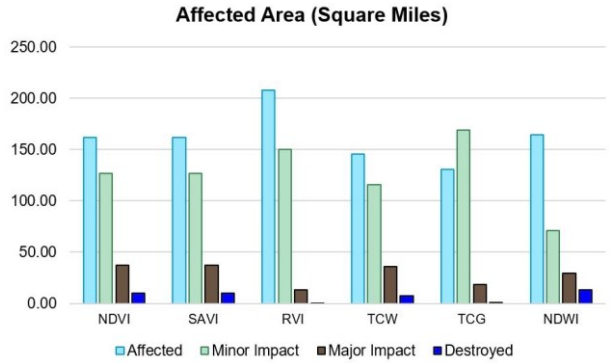


Figure 8. Affected area assessment

A further study is conducted into area estimates for the damage severity maps. Figure 8 presents a comparative assessment of the total area affected by Helene. NDVI, SAVI, and NDWI demonstrate a greater capacity to identify severe and extensive damage compared to other indices, revealing the most significant areas of destruction and considerable impact. TCG is notably responsive to major impact areas, identifying an extensive area of 167.23 square miles, indicating its proficiency in recognizing regions with substantial damage. RVI appears to identify small impact areas most effectively, detecting the biggest area of 205.32 square miles. The discovery indicates that RVI may prioritize the detection of minor harm and possibly exhibit reduced sensitivity to more severe effects. TCG and RVI indicate the most extensive regions of unaffected land, indicating that these models may adopt a more conservative approach in recognizing affected areas. The area of the impacted land varied between 130 square miles and 210 square miles (Figure 8).

## 5. Conclusions

This study conducted a thorough evaluation of the forest regions disrupted by Hurricane Helene in western North Carolina, utilizing different spectral indices and the UID algorithm with Landsat 8 data. The index-wise severity impact was assessed and corroborated by independent GIS data and ground samples. The statistical study and comparison of damage severity indicated that the NDWI change detection map was the most effective index among six regularly utilized indices, including NDVI, SAVI, TCW, and RVI for identifying hurricane-induced changes. The majority of the impacted forest regions had light to moderate damage severity. The accuracy assessments demonstrated that the composite index technique outperformed the separate spectral indices, with an overall accuracy of 86.53%. Given that our severity thresholds in the change detection maps were chosen based on the statistical characteristics of the data, it is likely that the thresholds in other cases may vary; such enhancements might extend the applicability of this method to more post-disturbance assessments. The time series analysis with high-resolution images could be a future direction to refine the findings.

## References

Ansari, R.A., Esimaje, T., Ibrahim, O.M. and Mulrooney, T., 2025. Analysis of Forest Change Detection Induced by Hurricane Helene Using Remote Sensing Data. *Forests*, *16*(5), p.788.

Cooper, R., 2024. Hurricane Helene Recovery. Office of State Budget and Management, December 13. Accessed: May 20, 2025. [Online]. Available: https://www.osbm.nc.gov/hurricane-helene-dna/open

Coppin, P., Jonckheere, I., Nackaerts, K., Muys, B. and Lambin, E., 2004. Review ArticleDigital change detection methods in ecosystem monitoring: a review. International journal of remote sensing, 25(9), pp.1565-1596., doi:10.1080/0143116031000101675.

Crist, E., 1986. Vegetation and soils information contained in transformed Thematic Mapper data. In Proceedings of IGARSS'86 Symposium (Vol. 1465). European Space Agency, Paris, pp. 1465-70.

Gao, B.C., 1996. NDWI—A normalized difference water index for remote sensing of vegetation liquid water from space. Remote sensing of environment, 58(3), pp.257-266., https://doi.org/10.1016/S0034-4257(96)00067-3.

He, H., Yan, J., Liang, D., Sun, Z., Li, J. and Wang, L., 2024. Time-series land cover change detection using deep learning-based temporal semantic segmentation. Remote Sensing of Environment, 305, p.114101.

Jing, W., Chi, K., Li, Q. and Wang, Q., 2025. ChangeRD: A registration-integrated change detection framework for unaligned remote sensing images. ISPRS Journal of Photogrammetry and Remote Sensing, 220, pp.64-74.

Kuzu, R.S., Antropov, O., Molinier, M., Dumitru, C.O., Saha, S. and Zhu, X.X., 2024. Forest disturbance detection via self-supervised and transfer learning with sentinel-1&2 images. IEEE Journal of Selected Topics in Applied Earth Observations and Remote Sensing, 17, pp.4751-4767., doi: 10.1109/JSTARS.2024.

Liu, S., Marinelli, D., Bruzzone, L. and Bovolo, F., 2019. A review of change detection in multitemporal hyperspectral images: Current techniques, applications, and challenges. IEEE Geoscience and Remote Sensing Magazine, 7(2), pp.140-158., https://doi.org/10.1109/MGRS.2019.2898520

Lu, M., 2025. Dimension Expansion-based Spatiotemporal Land Cover Change Detection: A Study Case Using Sentinel-2 Satellite Time Series. The International Archives of the Photogrammetry, Remote Sensing and Spatial Information Sciences, 48, pp.29-34.

Lv, Z., Liu, T., Zhang, P., Atli Benediktsson, J. and Chen, Y., 2018. Land cover change detection based on adaptive contextual information using bi-temporal remote sensing images. Remote Sensing, 10(6), p.901. https://doi.org/10.3390/rs10060901

NHQRedCrossGIS, "DDA-Collect for DR 215-25 Hurricane Helene NC/SC 09/24 HUR - Feature Layer - Partner View", Accessed: Nov. 3, 2024. [Online.] Available: https://services.arcgis.com/pGfbNJoYypmNq86F/arcgis/rest/services/DDAC_DR_215_25_Hurricane_Helene_NC_SC_0924_HUR_Partner_View/FeatureServer.

NLCD (National Land Cover Database). Annual NLCD 2023. "National Land Cover Database", Accessed: Dec. 28, 2024. [Online.] Available: https://www.mrlc.gov/data/project/annual-nlcd

Pulvirenti, L., Squicciarino, G. and Fiori, E., 2020. A method to automatically detect changes in multitemporal spectral indices: Application to natural disaster damage assessment. Remote Sensing, 12(17), p.2681., https://doi.org/10.3390/rs12172681.

Rouse J.W. Hass, R.H., Schell J.A. and Deering D.W.., 1973. Monitoring vegetation systems in the great plains with ERTS. In Third NASA Earth Resources Technology Satellite Symposium, 1973 (Vol. 1, pp. 309-317).

Rynkiewicz, A., Hościło, A., Aune-Lundberg, L., Nilsen, A.B. and Lewandowska, A., 2025. Detection and quantification of vegetation losses with Sentinel-2 images using bi-temporal analysis of spectral indices and transferable random forest model. Remote Sensing, 17(6), p.979. https://doi.org/10.3390/rs17060979

Salim, M.Z., Al Kafy, A., Altuwaijri, H.A., Miah, M.T., Jodder, P.K. and Rahaman, Z.A., 2024. Quantitative assessment of Hurricane Ian's damage on urban vegetation dynamics utilizing Landsat 9 in Fort Myers, Florida. Physics and Chemistry of the Earth, Parts A/B/C, 136, p.103750. https://doi.org/10.1016/j.pce.2024.103750.

Singh, G., Dahiya, N., Sood, V., Singh, S. and Sharma, A., 2024. ENVINet5 deep learning change detection framework for the estimation of agriculture variations during 2012–2023 with Landsat series data. Environmental Monitoring and Assessment, 196(3), p.233.

United States Census Bureau, "McDowell County, North Carolina", Accessed: June. 20, 2025. [Online.] Available: https://data.census.gov/

Wu, K., Chen, T., Xu, Y., Song, D. and Li, H., 2021. A novel change detection approach based on spectral unmixing from stacked multitemporal remote sensing images with a variability of endmembers. Remote Sensing, 13(13), p.2550. https://doi.org/10.3390/rs13132550

Zhao, C., Pan, Y., Wu, H., Ren, S., Ma, G., Gao, Y., Zhu, Y. and Jing, G., 2024. A novel spectral index for vegetation destruction event detection based on multispectral remote sensing imagery. IEEE Journal of Selected Topics in Applied Earth Observations and Remote Sensing, 17, pp.11290-11309. doi: 10.1109/JSTARS.2024.3412737.

Zhou, M., Li, D., Liao, K. and Lu, D., 2023. Integration of Landsat time-series vegetation indices improves consistency of change detection. International Journal of Digital Earth, 16(1), pp.1276-1299.